

Mass Spectrometric Studies of the Effect of pH on the Accumulation of Intermediates in Denitrification by *Paracoccus denitrificans*

JENS K. THOMSEN, TORBEN GEEST, AND RAYMOND P. COX*

Institute of Biochemistry, Odense University, DK-5230 Odense M, Denmark

Received 7 June 1993/Accepted 20 November 1993

We have used a quadrupole mass spectrometer with a gas-permeable membrane inlet for continuous measurements of the production of N_2O and N_2 from nitrate or nitrite by cell suspensions of *Paracoccus denitrificans*. The use of nitrate and nitrite labeled with ^{15}N was shown to simplify the interpretation of the results when these gases were measured. This approach was used to study the effect of pH on the production of denitrification intermediates from nitrate and nitrite under anoxic conditions. The kinetic patterns observed were quite different at acidic and alkaline pH values. At pH 5.5, first nitrate was converted to nitrite, then nitrite was converted to N_2O , and finally N_2O was converted to N_2 . At pH 8.5, nitrate was converted directly to N_2 , and the intermediates accumulated to only low steady-state concentrations. The sequential usage of nitrate, nitrite, and nitrous oxide observed at pH 5.5 was simulated by using a kinetic model of a branched electron transport chain in which alternative terminal reductases compete for a common reductant.

Denitrification is the bacterial conversion of nitrate and nitrite to the gaseous products, N_2O and N_2 . The microorganisms concerned (30) use the nitrogenous oxidants as alternative terminal acceptors for a branched electron transport system (25). In natural ecosystems, nitrate is the usual substrate, and it is often converted to N_2 without appreciable accumulation of intermediates (27). However, there are also reports of nitrous oxide accumulation in the presence of low oxygen concentrations (27) or in acidic environments (15, 23). Low pH values were also observed to cause the transient production of N_2O by cell suspensions of *Paracoccus denitrificans* in the study of Kučera et al. (19). They observed appreciable accumulation at pH 6.4 but not at pH 7.4. Accumulation of nitrite as the result of denitrification has also been observed (3, 4).

A complete picture of the kinetics of denitrification requires information about the time-dependent changes in concentration of all the nitrogenous compounds. Mass spectrometry in combination with an inlet with a gas-permeable membrane allows continuous measurements of all dissolved gases (10, 11), making it easy to monitor not only N_2O and N_2 but also O_2 and CO_2 as a measure of the breakdown of organic substrates. This technique is ideally suited for studies of denitrification (7, 9, 14, 20, 21).

We report here details of the techniques that we have developed for such studies, particularly the use of substrates labeled with the stable isotope ^{15}N combined with separate determinations of nitrate and nitrite, and investigations of effect of pH on the patterns of intermediate formation during the reduction of nitrate, nitrite, and nitrous oxide by *P. denitrificans*.

MATERIALS AND METHODS

Growth of bacteria. *P. denitrificans* DSM 413 was obtained from the Deutsche Sammlung von Mikroorganismen und Zellkulturen, Braunschweig, Germany.

* Corresponding author. Mailing address: Institute of Biochemistry, Odense University, Campusvej 55, DK-5230 Odense M, Denmark. Phone: +45 66 15 86 00. Fax: +45 65 93 03 52.

All experiments were performed with cells taken directly from a nitrate-limited continuous culture in the steady state. The incoming medium contained 25 mM succinic acid, 25 mM Tris base, 25 mM KOH, 25 mM $NaNO_3$, 5 mM $(NH_4)_2SO_4$, a solution (10 ml/liter) containing 10 g of $MgCl_2 \cdot 6H_2O$ per liter and 2.5 g of $CaCl_2 \cdot 2H_2O$ per liter, 2 ml of 1.0 M potassium phosphate (pH 7.0) per liter, 2 ml of the trace element solution SL-6 (22) per liter, and a solution (2 ml/liter) containing 100 mM $FeCl_3$ and 200 mM EDTA.

The bioreactor used was similar to that described by Iversen et al. (12). The temperature was maintained at 30°C. The culture volume was 500 ml, and the headspace was gassed with N_2 . The culture was diluted at $0.2 h^{-1}$ with medium in equilibrium with air. The cell concentration was continually monitored by circulating the culture through a measuring chamber with a light-emitting diode-photodiode (8). The steady-state cell concentration corresponded to about 500 mg of cell carbon per liter, and the culture supernatant contained 30 μM nitrite and less than 5 μM nitrate. The incoming medium was designed such that bacterial metabolism caused the pH of the bioreactor contents to increase to pH 8.5 in the steady state.

The cells were harvested by centrifugation at $10,000 \times g$ for 10 min, resuspended in the same volume of medium containing 20 mM *N*-2-hydroxyethylpiperazine-*N'*-2-ethanesulfonic acid (HEPES), 10 mM succinic acid, 20 mM NaOH, and 1 mM $MgCl_2$ adjusted to pH 7.5 with KOH, and centrifuged again. The final pellet was resuspended in a small volume of the same medium and used immediately.

Cell carbon was measured with a total organic carbon analyzer. Cell concentration was routinely measured by turbidimetry at 550 nm after appropriate dilution, and the apparent absorbance was converted to milligrams of cell carbon per liter by using a calibration factor.

Activity measurements. Changes in the concentrations of dissolved gases were measured by using a quadrupole mass spectrometer (Dataquad DQ100 [Spectrum Scientific, Runcorn, United Kingdom] or HAL 100 [Hiden Analytical, Warrington, United Kingdom]) equipped with a membrane introduction probe manufactured in our workshop. The inlet consists of a 2-mm-inside-diameter stainless steel tube with

one end closed and the other connected to the mass spectrometer by a length of flexible vacuum tubing. The walls of the tube contain several (typically 10) circular holes 0.4 mm in diameter which are covered by a length of narrow-bore silicon rubber tubing (Silastic; Dow-Corning) with 1.47-mm inside diameter and an unstretched wall thickness of 0.25 mm. A 90% response was typically obtained after 40 s when measurements were performed at 30°C in water.

The inlet probe was inserted through the stopper of a Plexiglas reaction vessel (nominal volume, 12 ml) equipped with a water jacket allowing the temperature to be maintained at 30°C. The stopper had a central capillary tube connected to the apex of the conical lower surface and an external screw thread with a collar allowing its position to be adjusted. This allowed bubbles of gas to be removed from the cell suspension and samples to be removed through an injection needle while the volume of the chamber was simultaneously adjusted to minimize contact of the contents with atmospheric O₂. It also permitted known volumes of gases to be added by allowing them to dissolve from a bubble at the end of an injection needle. The basic design of the inlet probe and reaction vessel have been described in more detail by Cox (6) and Jensen and Cox (13).

The mass spectrometer signals at up to 4 *m/z* values were captured at 30-s intervals by a desktop computer (Acorn Archimedes [Acorn, Cambridge, United Kingdom] or IBM-compatible personal computer), using specially written programs.

Bacteria were suspended in a reaction medium containing 10 mM succinic acid, 20 mM NaOH, 1 mM MgCl₂, and 20 mM buffer adjusted to the appropriate pH with KOH. Succinate was used as buffer at pH 5.5, 2-(*N*-morpholino)ethanesulfonic acid (MES) was used at pH 6.0 and 6.5, 3-(*N*-morpholino)propanesulfonic acid (MOPS) was used at pH 7.0, HEPES was used at pH 7.5, *N*-tris(hydroxymethyl)methyl-3-aminopropanesulfonic acid (TAPS) was used at pH 8.5, and glycine was used at pH 9.5. Experiments were usually started by adding a small volume of concentrated cell suspension to air-saturated medium and allowing the bacteria to remove O₂ by respiration before the addition of nitrogenous oxidants.

In experiments in which nitrate or nitrite labeled with ¹⁵N was added as an oxidant, ¹⁵N₂O was measured at *m/z* = 46 and ¹⁵N₂ was measured at *m/z* = 30 after subtraction of the calculated signal from the ¹⁵N₂⁺ fragment from ¹⁵N₂O. In experiments in which ¹⁴N₂O was added as an oxidant, consumption of ¹⁴N₂O was measured at *m/z* = 30 and the ¹⁴N₂ produced was measured at *m/z* = 14 after subtraction of the calculated signal from the ¹⁴N⁺ fragment from ¹⁴N₂O. O₂ was measured at *m/z* = 32, and CO₂ was measured at *m/z* = 44. All calibrations were made by using the solubility data given by Wilhelm et al. (29). The signals due to N₂ and O₂ were calibrated with air-saturated buffer at 30°C. Calibration of the N₂O signals and determination of the fraction of the signal from the molecular ion corresponding to the N₂⁺ and N⁺ peaks were made by measuring the increase in signal at *m/z* values of 14, 28, 30, and 44 obtained by dissolving known volumes of ¹⁴N₂O gas in degassed buffer at 30°C, using a gastight syringe.

Nitrate and nitrite in cell suspensions were measured by using samples (100 μl) removed from the reaction vessel, quenched by dilution into 400 μl of ice-cold 10 mM NaOH, and frozen in liquid nitrogen before storage at -20°C. The samples were carefully thawed and either passed through a 0.2-μm-pore-size filter or centrifuged at 15,000 × *g* for 4 min at 4°C to remove the cells. Nitrate and nitrite were either determined colorimetrically, using an autoanalyzer in which

part of the sample was reduced on a cadmium column, or by high-pressure liquid chromatography (HPLC) with direct UV detection, using 20 mM sodium methanesulfonate as the eluent and a Wescan Anion/R column (30 by 4.6 mm [inside diameter]) as the only column (26).

Computer simulation. Simulations were carried out on an Acorn A5000 desktop computer with a program in structured BASIC, using the ODEINT routine with variable step-size fifth-order Runge-Kutta integration as given by Sprott (24).

RESULTS

Simultaneous mass spectrometric measurements of N₂, N₂O, O₂, and CO₂. Gas molecules which diffuse into the vacuum system of a mass spectrometer are broken down into a characteristic pattern of ions which are then separated according to their mass/charge ratio to produce a mass spectrum. Thus, N₂O shows peaks corresponding to N₂O⁺, the molecular ion, and also the fragments N₂⁺, NO⁺, N⁺, and O⁺ (5). In addition to the major ions corresponding to ¹⁴N and ¹⁶O, there will be smaller peaks corresponding to the natural abundance of other isotopes of nitrogen and oxygen. The quadrupole mass spectrometers which we use are incapable of distinguishing between peaks due to ions with the same integer *m/z* but different atomic compositions; therefore, N₂ is not separated from CO⁺. The interpretation of spectra corresponding to a mixture of gases is thus potentially complex because an individual peak does not necessarily correspond exclusively to a particular compound.

The problem of overlapping mass spectra can in principle be solved by computation by solving a set of simultaneous equations, as long as the fragmentation patterns for the individual components are accurately known and there are at least as many peaks as components. However, we have found that the problems can be considerably reduced if the stable isotope ¹⁵N is used. This allows unambiguous determination of ¹⁵N₂O at *m/z* = 46, CO₂ at *m/z* = 44, and O₂ and *m/z* = 32. The only correction needed is for measurement of ¹⁵N₂ in the presence of ¹⁵N₂O, in which case the fraction of the signal at *m/z* = 46 corresponding to the N₂⁺ peak of ¹⁵N₂O at *m/z* = 30 must be subtracted. This is easy to do if the data are collected by computer and will be a potential source of significant errors only if N₂O is present at higher concentrations than N₂.

A further advantage of the use of ¹⁵N is that N₂ production due to microbial activity can be observed without any background due to atmospheric N₂. High sensitivity can thus be obtained without the precautions which would be needed to avoid atmospheric N₂ both in the suspension medium and in the residual vacuum of the mass spectrometer.

Measurements of carbon dioxide are potentially of great value as a monitor of substrate metabolism. However, the mass spectrometer signal is sensitive only to dissolved CO₂, since HCO₃⁻ cannot diffuse through the membrane. Thus, it is difficult to measure inorganic carbon at pH values much above the pK_a of about 6.4. At neutral and alkaline pH values, the signal due to CO₂ is also very sensitive to pH, and reliable measurements are possible only in well-buffered medium. The mass spectrometer also shows a significant background signal due to CO₂, which further limits sensitivity.

Figure 1 shows an example of the results obtained with use of mass spectrometry to measure dissolved gases in a suspension of denitrifying bacteria. A washed cell suspension of *P. denitrificans* was added to air-saturated buffer at pH 8.5 containing ¹⁵N-nitrate in a closed reaction vessel. To provide a

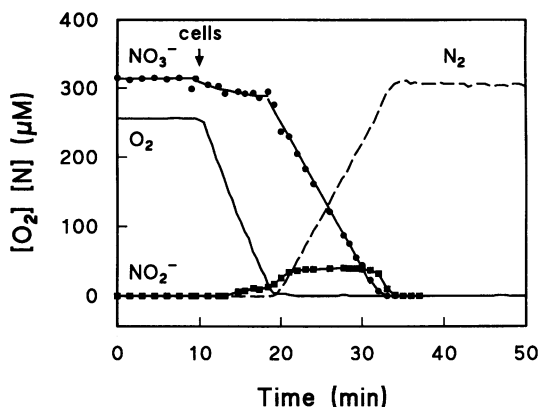


FIG. 1. Changes in dissolved gases, nitrate, and nitrite in a suspension of *P. denitrificans* at pH 8.5. The cell concentration corresponded to 90 mg of cell carbon per liter. Nitrate and nitrite were determined by HPLC. The concentration of N_2O (not shown) remained less than $3 \mu\text{M N}$ throughout the experiment. All nitrogen compounds are shown as micromolar N.

complete picture of the progress of the reaction, the ionic components were determined by HPLC after carefully removing samples while retaining anoxic conditions in the reaction vessel.

At pH 8.5, close to the pH in the chemostat during growth, only a small decrease in nitrate concentration and increase in nitrite was observed until O_2 was consumed. Nitrate consumption started immediately anoxic conditions were attained, while nitrite increased to a concentration of about $40 \mu\text{M}$ and remained in a steady state until nitrate was consumed. N_2 increased as nitrate fell. N_2O concentrations did not rise above values distinguishable from zero on Fig. 1, where all components are shown on the same scale.

The sum of the observed nitrogenous compounds remained essentially constant throughout the experiment. The small downward trend is the result of loss of material into the mass spectrometer vacuum. This is unavoidable when a probe with a large membrane surface area is used together with a reaction vessel with a small volume.

Effect of pH on denitrification kinetics under anoxic conditions. We investigated the effects of pH in the range between 5.5 and 9.5 in experiments in which nitrate was added after anoxic conditions were obtained. At more acidic pH values, the kinetic patterns observed became more complex than the simple conversion of nitrate to N_2 observed at pH 8.5. The most extreme pattern was observed at pH 5.5 (Fig. 2). Here the utilization of nitrogenous substrates was essentially sequential, and the reaction could be divided into three distinct phases. In phase I, nitrate was converted to nitrite and a small amount of N_2O ; this phase ended when nitrate became undetectable. In phase II, the nitrite which had accumulated in almost stoichiometric amounts was converted to N_2O . Phase II ended when nitrite was removed. No N_2 production was detected until phase III, when the accumulated N_2O was converted to N_2 . The rates of change of all components were essentially constant (zero-order kinetics), and there was no evidence for any limitation by substrate concentrations above values around $10 \mu\text{M}$. We confirmed in separate experiments in the absence of cells that chemical breakdown of nitrite was not contributing to its disappearance at pH 5.5.

At pH values above 5.5, the kinetic patterns were intermediate between those in Fig. 1 and 2. At pH 6.5, phases I and II

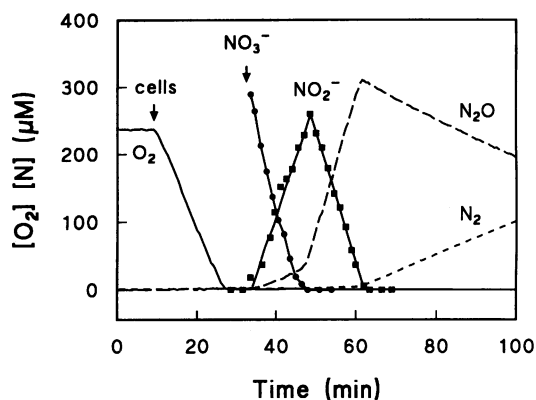


FIG. 2. Changes in dissolved gases, nitrate, and nitrite in a suspension of *P. denitrificans* at pH 5.5. The cell concentration corresponded to 118 mg of cell carbon per liter. Nitrite and nitrate were determined by autoanalyzer. All nitrogen compounds are shown as micromolar N.

were combined, and nitrate was converted to N_2O . There was no nitrite peak, but a steady-state concentration of around $30 \mu\text{M}$ was maintained during phases I and II. As was observed at pH 5.5, there was a distinguishable phase III in which N_2O is converted to N_2 .

The patterns of intermediate production observed at pH values between 5.5 and 8.5 are summarized in Fig. 3. For each

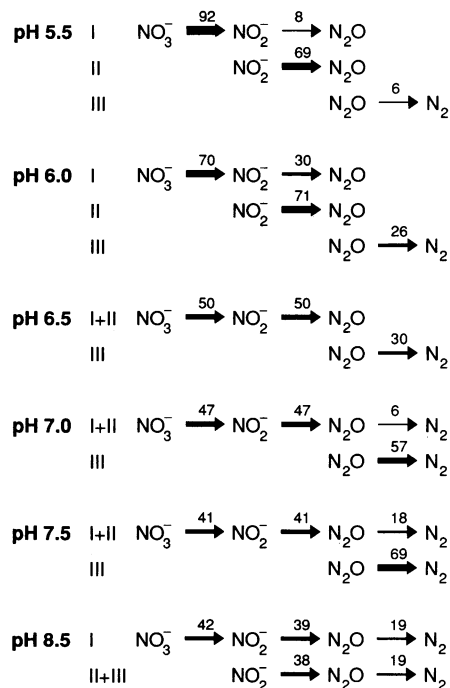


FIG. 3. Scheme showing the rates of different partial reactions during the conversion of nitrate to N_2 at different pH values. The end of phase I corresponds to the time when all nitrate is removed (similarly for phase II and nitrite and phase III and N_2O). The thickness of the arrows is proportional to the flux of reducing equivalents, normalized to the total flux during phase I; the numbers above the arrows show these values as percentages. (To obtain comparable rates of nitrogen conversion, the values for the conversion of N_2O to N_2 should be multiplied by 2.)

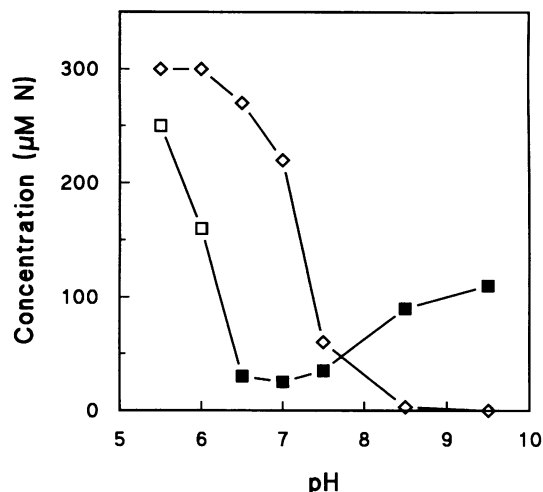


FIG. 4. Effect of pH on the maximum concentrations of intermediates observed during the conversion of 300 μM nitrate to N_2 . \square , maximum concentration of nitrite at the end of phase I; \blacksquare , steady-state concentration of nitrite during phase I; \diamond , maximum concentration of nitrous oxide at the end of phase II.

phase and pH value, the rate of each partial reaction is given as a percentage of the total flux of reducing equivalents during phase I at that pH. Nitrogen conversion rates can be obtained by multiplying the reductant flux for conversion of N_2O to N_2 by 2. If the generating reaction has a greater nitrogen conversion rate than the consuming reaction does during a particular phase, the intermediate will accumulate. Starting from acid pH values, there is first a clear trend toward decreased accumulation of nitrite during phase I, until phases I and II are indistinguishable at pH 6.5. As the pH is further increased, N_2 begins to accumulate while nitrate is present, resulting in decreased accumulation of N_2O at the end of phase II. The maximum concentration of intermediates observed are shown in Fig. 4.

At pH 8.5, a steady-state concentration of nitrite is rapidly attained on adding nitrate and remains fairly constant until nitrate is exhausted (end of phase I). There is thus a short but distinguishable phase corresponding to a combination of phases II and III, when nitrite is converted to N_2 without the accumulation of N_2O .

The kinetic pattern observed at pH 9.5 resembles that at pH 8.5 except that the steady-state concentration of nitrite observed until the point where nitrate was almost consumed was higher. This is shown in Fig. 4 as an increase in the maximum concentration observed after a minimum at neutral pH values; the cause of this accumulation is obviously qualitatively different from the cause of the sharp peaks observed at acid pH values.

A second series of experiments was performed in which the reaction was started by adding ^{15}N -nitrite instead of nitrate. At acid pH values, the expected accumulation of N_2O was observed. The rates of the two partial reactions involved are summarized in Fig. 5.

The observation of high nitrite concentrations in an apparent steady state at high pH values suggests that the affinity of the cells for nitrite may be quite low under these conditions. At acid and neutral pH values, the disappearance of nitrite was zero order until the concentration was under 10 μM . At pH 7.5 and above, the loss of nitrite and appearance of gaseous products showed clearly decreasing rates as the nitrite concen-

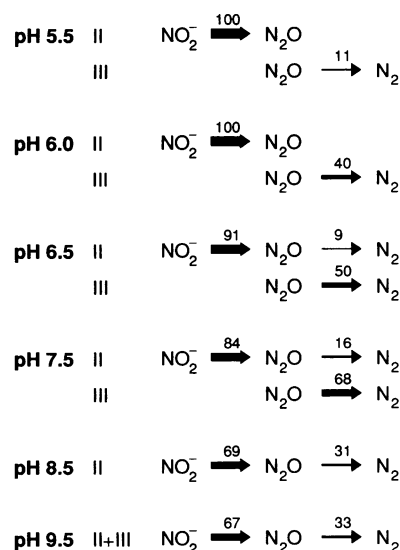


FIG. 5. Scheme showing the rates of different partial reactions during the conversion of nitrite to N_2 at different pH values. The definitions of phases II and III are the same as for Fig. 3. The thickness of the arrows is proportional to the flux of the reducing equivalents normalized to the total flux during phase II; these values are shown above the arrows as percentages. (To obtain comparable rates of nitrogen conversion, the values for the conversion of N_2O to N_2 should be multiplied by 2.)

tration fell; this effect became much more pronounced as pH increased. The results at pH 9.5 (not shown) were analyzed by differentiating the progress curves and fitting the resulting rate-concentration data to the Michaelis-Menten equation. The results gave a good fit, with a K_m value of 28 μM .

The effects of pH on the rates of the three individual reactions of denitrification are summarized in Fig. 6. The values correspond to the rates observed in phase I for nitrate and phase II for nitrite. Rates for N_2 production from N_2O at low pH values were obtained from phase III in the experimental series initiated by addition of nitrate or nitrite. At high pH values, N_2 production was measured in experiments in which the reaction was started by adding a small volume of N_2O -saturated buffer to the bacterial suspension. The values for nitrate and nitrite are shown both as rates of concentration change and as rates of reductant consumption, calculated from knowledge of the products being formed; the two measures are identical for N_2O , which has only one possible product. The rate of oxygen uptake is also shown as rate of reductant consumption. These results show that the cells have a potential capacity for reductant generation which is in excess of the observed rates of utilization of all of the nitrogenous oxidants. Similar results were obtained from the analysis of CO_2 production rates at acidic pH values (not shown).

DISCUSSION

The kinetic patterns observed in experiments of the type reported here depend on the relative activities of the various enzymes with their own substrates and the possible inhibitory effects of alternative substrates. Patterns such as those observed at alkaline pH values at which intermediates accumulate to lower steady-state values are expected if the K_m for intermediates is quite low, the V_{max} for intermediates is greater than for the original substrate, and reductases are not inhibited

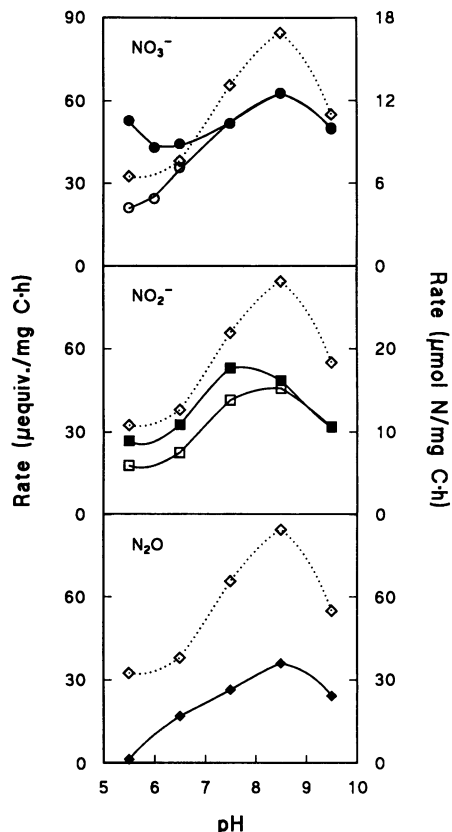


FIG. 6. Effect of pH on the rates of reduction of nitrate, nitrite, and N_2O . Rates for nitrate and nitrite are shown both as change in concentration under zero-order conditions (\bullet , \blacksquare) and as the equivalent rate of reductant utilization (\circ , \square). The scales corresponding to reductant utilization are multiplied by 5 in the case of nitrate and by 3 in the case of nitrite, so that complete conversion to N_2 results in two superimposed values. The dotted line shows the rate of reductant utilization when O_2 was the electron acceptor, before the addition of nitrate (\diamond).

by the presence of alternative oxidants. Thus, the simple sequential model suggested by Betlach and Tiedje (3, 27), which involves only the K_m values for the nitrogenous oxides and the V_{max} values for the various reductases, could explain the observed results.

In contrast, a sequential pattern such as that observed at acidic pH values cannot be explained by a model which does not consider inhibitory effects of one substrate on the utilization of a second. A series of intermediates accumulating to essentially stoichiometric concentrations will be observed in a sequential reaction process only if the maximal rate of each successive reaction is much slower than the preceding one, and this is clearly not the case here for nitrate and nitrite at acidic pH values.

The mechanisms involved in interactions between alternative acceptors in denitrifying *P. denitrificans* have been investigated by Alefounder and coworkers (2) and by Kučera and coworkers (17, 18). Such control phenomena are observed even at neutral pH values when two nitrogenous acceptors are added or when O_2 is used rather than nitrate, nitrite, or nitrous oxide. There is some experimental evidence supporting the idea that control is exerted via the redox level of common components at the two branch points, ubiquinol/ubiquinone

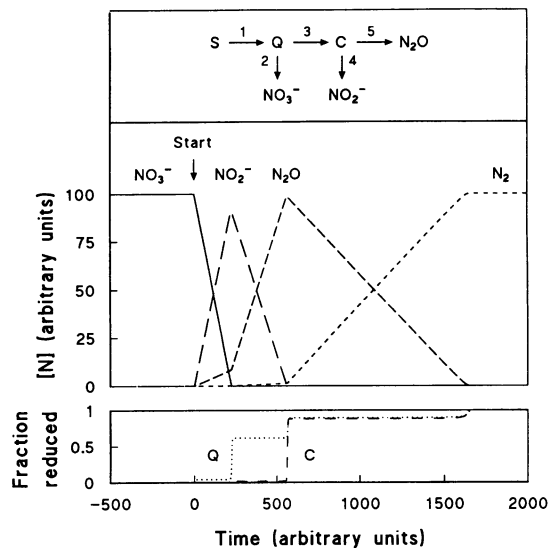


FIG. 7. Results of a computer simulation of intermediate formation during the conversion of nitrate to N_2 . The model used involved five two-substrate enzyme reactions (V_{max} and the two K_m values K_D for the electron donor and K_A for the acceptor in parentheses): $S \rightarrow Q$ ($K_{D1} = 1, K_{A1} = 1, V_1 = 1$); $QH_2 \rightarrow$ nitrate ($K_{D2} = 1, K_{A2} = 0.05, V_2 = 1$); $QH_2 \rightarrow C_{ox}$ ($K_{D3} = 1, K_{A3} = 1, V_3 = 1$); $C_{red} \rightarrow$ nitrite ($K_{D4} = 1, K_{A4} = 0.05, V_4 = 1$); and $C_{red} \rightarrow$ nitrous oxide ($K_{D5} = 1, V_{A5} = 1, V_5 = 0.2$). The S concentration was maintained constant at 100, and the sum of the oxidized and reduced forms of Q and C was maintained at 1.0. The reaction rate v was calculated by using the expression of Alberty (1): $v = (V[A][B]) / (K_A[B] + K_D[A] + [A][B])$.

for nitrate reductase versus nitrite and nitrous oxide reductases and cytochrome *c* for nitrite versus nitrous oxide reductases. Kučera et al. (17) observed changes in the redox level of cytochrome *c* during the sequential utilization of an added mixture of nitrite and nitrate, and Alefounder et al. (2) reported indirect evidence for changes in the ratio between ubiquinol and ubiquinone measured through the redox level of *b*-type cytochromes and quenching of the fluorescence due to anthryloxy stearic acid.

The patterns of intermediate accumulation which we observed experimentally can be reproduced by a model (Fig. 7) which involves a doubly branched electron transport pathway with five reactions and two branch points with common mobile electron carriers Q (ubiquinone/ubiquinol) and C (cytochrome *c*). The rate of each reaction was assumed to depend on the concentration of its two substrates, and from several possible mathematical relationships, we arbitrarily selected the equation of Alberty (1) for a two-substrate enzyme reaction.

The patterns observed at different pH values can be qualitatively simulated by appropriate combinations of the parameters. Figure 7 shows a pattern which resembles the experimental results at pH 5.5 (Fig. 1). The simulation also reproduces the experimentally observed decrease in electron flux between phase I and phase II (Fig. 3).

The values of most of the parameters in our model are chosen arbitrarily and have no particular relation to the actual kinetic constants within the bacterial cell. Our results thus demonstrate only that it is possible to obtain the observed patterns with a kinetic model of this type, without the need to postulate separate allosteric interactions.

Figure 7 also shows the redox level of Q and C predicted by the model during the course of the process, showing the

expected shift in reduction level as the reaction shifts from the high-affinity branch to the low-affinity branch. The magnitude of these changes is greater than those observed experimentally (2, 17). However, the model makes no pretence of being able to make quantitative predictions of this type.

It is noteworthy that the transient accumulation of nitrous oxide at low pH values, which seems to be commonly observed in natural environments, does not necessarily result from competition for common intermediates. If the maximum rate of nitrous oxide reduction is less than the rate of nitrite reduction, then nitrous oxide will accumulate. In this case, however, the alternative acceptors will be reduced in parallel at rates which are independent of the presence of competitive oxidants, as observed, for example, by Betlach and Tiedje (3).

We observed (Fig. 6) that low pH values have a much greater inhibitory effect on nitrous oxide reduction (phase III) than on nitrite reduction (phase II). This finding is in agreement with the properties of the purified enzymes (16, 28), as expected since both enzymes are periplasmic and thus exposed to the same pH as the environment of intact bacteria.

The experiments reported here demonstrate the value of mass spectrometry combined with a membrane introduction probe for measurements of denitrification and related gas exchange reactions. In combination with a nitrate-sensitive electrode, the approach would allow all of the intermediates involved in denitrification except for nitrite to be monitored continuously. The major potential limitation is the possibility that the peak at a given m/z value may contain contributions from more than one molecular species, but we have shown here how this can be largely eliminated by the use of substrates containing ^{15}N .

ACKNOWLEDGMENTS

This research was supported by the Carlsberg Foundation, the Danish Council for Scientific and Industrial Research, and Direktør Ib Henriksens Fond.

REFERENCES

1. **Alberty, R. A.** 1953. Relationship between Michaelis constants, maximum velocities and the equilibrium constant for an enzyme-catalyzed reaction. *J. Am. Chem. Soc.* **75**:1928–1932.
2. **Alefounder, P. R., A. J. Greenfield, J. E. G. McCarthy, and S. J. Ferguson.** 1983. Selection and organisation of denitrifying electron-transfer pathways in *Paracoccus denitrificans*. *Biochim. Biophys. Acta* **724**:20–39.
3. **Betlach, M., and J. M. Tiedje.** 1981. Kinetic explanation for accumulation of nitrite, nitric oxide and nitrous oxide during bacterial denitrification. *Appl. Environ. Microbiol.* **42**:1074–1084.
4. **Carlson, C. A., and J. L. Ingraham.** 1983. Comparison of denitrification by *Pseudomonas stutzeri*, *Pseudomonas aeruginosa*, and *Paracoccus denitrificans*. *Appl. Environ. Microbiol.* **45**:1247–1253.
5. **Cornu, A., and R. Massot.** 1966. Compilation of mass spectral data. Heyden & Son Ltd., London.
6. **Cox, R. P.** 1987. Membrane inlets for on-line liquid-phase mass spectrometric measurements in bioreactors, p. 63–74. *In* E. Heinze and M. Reuss (ed.), *Mass spectrometry in biotechnological process analysis and control*. Plenum Press, New York.
7. **Cox, R. P., T. Geest, and J. K. Thomsen.** 1990. Kinetics of denitrification in *Paracoccus denitrificans*: measurements using ^{15}N -nitrate and a mass spectrometer with a permeable membrane inlet. *Mitt. Dtsch. Bodenkundl. Ges.* **60**:307–312.
8. **Cox, R. P., M. Miller, J. B. Nielsen, M. Nielsen, and J. K. Thomsen.** 1989. Continuous turbidometric measurements of microbial cell density in bioreactors using a light-emitting diode and a photodiode. *J. Microbiol. Methods* **10**:25–31.
9. **Davies, K. J. P., D. Lloyd, and L. Boddy.** 1989. The effect of oxygen on denitrification in *Paracoccus denitrificans* and *Pseudomonas aeruginosa*. *J. Gen. Microbiol.* **135**:2445–2451.
10. **Degn, H.** 1991. Membrane inlet mass spectrometry in pure and applied microbiology. *J. Microbiol. Methods* **15**:185–197.
11. **Degn, H., R. P. Cox, and D. Lloyd.** 1985. Continuous measurements of dissolved gasses in biochemical systems with the quadrupole mass spectrometer. *Methods Biochem. Anal.* **31**:165–194.
12. **Iversen, J. J. L., M. Nielsen, and R. P. Cox.** 1989. Design and performance of a simple, inexpensive, modular laboratory-scale bioreactor. *Biotech. Educ.* **1**:11–15.
13. **Jensen, B. B., and R. P. Cox.** 1988. Measurements of hydrogen exchange and nitrogen uptake by mass spectrometry. *Methods Enzymol.* **167**:467–474.
14. **Jensen, K. M., and R. P. Cox.** 1992. Effects of sulfide and low redox potential on the inhibition of nitrous oxide reduction by acetylene in *Pseudomonas nautica*. *FEMS Microbiol. Lett.* **96**:13–18.
15. **Knowles, R.** 1982. Denitrification. *Microbiol. Rev.* **46**:43–70.
16. **Kristjansson, J. K., and T. C. Hollocher.** 1981. Partial purification and characterization of nitrous oxide reductase from *Paracoccus denitrificans*. *Curr. Microbiol.* **6**:247–251.
17. **Kučera, I., V. Dadák, and R. Dobrý.** 1983. The distribution of redox equivalents in the anaerobic respiratory chain of *Paracoccus denitrificans*. *Eur. J. Biochem.* **130**:359–364.
18. **Kučera, I., L. Lampardová, and V. Dadák.** 1987. Control of respiration rate in non-growing cells of *Paracoccus denitrificans*. *Biochem. J.* **246**:779–782.
19. **Kučera, I., R. Matyášek, and V. Dadák.** 1986. The influence of pH on the kinetics of dissimilatory nitrite reduction in *Paracoccus denitrificans*. *Biochim. Biophys. Acta* **848**:1–7.
20. **Lloyd, D., L. Boddy, and K. J. P. Davies.** 1987. Persistence of bacterial denitrification capacity under aerobic conditions: the rule rather than the exception. *FEMS Microbiol. Ecol.* **45**:185–190.
21. **Lloyd, D., K. J. P. Davies, and L. Boddy.** 1986. Mass spectrometry as an ecological tool for in-situ measurements of dissolved gasses in sediment systems. *FEMS Microbiol. Ecol.* **38**:11–17.
22. **Malik, K. A.** 1983. A modified method for the cultivation of phototrophic bacteria. *J. Microbiol. Methods* **1**:343–352.
23. **Nägele, W., and R. Conrad.** 1990. Influence of soil pH on the nitrate-reducing microbial populations and their potential to reduce nitrate to NO and N₂O. *FEMS Microbiol. Ecol.* **74**:49–58.
24. **Sprott, J. C.** 1991. Numerical recipes: routines and examples in BASIC. Cambridge University Press, Cambridge.
25. **Stouthamer, A. H.** 1991. Metabolic regulation including anaerobic metabolism in *Paracoccus denitrificans*. *J. Bioenerg. Biomembr.* **23**:163–185.
26. **Thomsen, J. K., and R. P. Cox.** 1990. Alkanesulphonates as eluents for the determination of nitrite and nitrate by ion chromatography with direct UV detection. *J. Chromatogr.* **521**:53–61.
27. **Tiedje, J. M.** 1988. Ecology of denitrification and dissimilatory nitrate reduction to ammonium, p. 179–244. *In* A. J. B. Zehnder (ed.), *Biology of anaerobic microorganisms*. Wiley, New York.
28. **Timkovich, R., R. Dhesi, K. J. Martinkus, M. K. Robinson, and M. R. Timothy.** 1982. Isolation of *Paracoccus denitrificans* cytochrome *cd₁*: comparative kinetics with other nitrite reductases. *Arch. Biochem. Biophys.* **215**:47–58.
29. **Wilhelm, E., R. Battino, and R. J. Wilcock.** 1977. Low-pressure solubility of gases in liquid water. *Chem. Rev.* **77**:219–262.
30. **Zumft, W. G.** 1992. The denitrifying prokaryotes, p. 554–582. *In* A. Balows, H. G. Trüper, M. Dworkin, W. Harder, and K.-H. Schleifer (ed.), *The prokaryotes*, 2nd ed. Springer, Berlin.